PHYSICAL REVIEW B **83**, 064407 (2011)

Sensitivity of the magnetic properties of the $ZnCr_2O_4$ and $MgCr_2O_4$ spinels to nonstoichiometry

S. E. Dutton,[1,*] Q. Huang,[2] O. Tchernyshyov,[3] C. L. Broholm,[3] and R. J. Cava[1]
[1]*Department of Chemistry, Princeton University, Princeton, New Jersey 08544, USA*
[2]*Center for Neutron Research, NIST, Gaithersburg, Maryland 20899, USA*
[3]*Department of Physics and Astronomy, The Johns Hopkins University, Baltimore, Maryland 21218, USA*
(Received 29 November 2010; published 11 February 2011)

We report that small amounts of metal atom nonstoichiometry are possible in the $ZnCr_2O_4$ and $MgCr_2O_4$ spinels. The nonstoichiometry, though less than 2%, significantly impacts T_N and the nature of the magnetic correlations above T_N. The $Zn_{1+x}Cr_{2-x}O_4$ spinel is particularly sensitive. While stoichiometric $ZnCr_2O_4$ displays antiferromagnetic short-range correlations in the susceptibility above T_N, ferromagnetic correlations are observed in nonstoichiometric, hole-doped $Zn_{1+x}Cr_{2-x}O_4$. The $Mg_{1+x}Cr_{2-x}O_4$ spinels are less profoundly affected by nonstoichiometry, though significant changes are also observed. We contrast the magnetic properties of $Zn_{1+x}Cr_{2-x}O_4$ and $Mg_{1+x}Cr_{2-x}O_4$ ($x = 0$, 0.02, 0.04) with those of materials with the equivalent amounts of isovalent nonmagnetic Ga^{3+} substituted on the Cr^{3+} site to separate the effects of static site disorder and hole doping.

DOI: 10.1103/PhysRevB.83.064407 PACS number(s): 75.50.Ee, 75.47.Lx, 61.05.fm, 71.70.Ej

I. INTRODUCTION

The $ZnCr_2O_4$, $MgCr_2O_4$, and $CdCr_2O_4$ spinels are among the most extensively studied geometrically frustrated magnetic systems.[1–12] Despite having a relatively simple crystal structure (Fig. 1, inset), with the Cr^{3+} ions forming a three-dimensional array of corner sharing tetrahedra, the low-temperature magnetostructural behavior is complex. All of the chromium (III) spinels undergo an antiferromagnetic ordering transition with $T_N < 13$ K, accompanied by a structural transition to lower crystallographic symmetry. Given the presence of isotropic spin Cr^{3+} (d^3), the lowering of symmetry is thought to be driven by spin-lattice coupling in a spin-Peierls-like transition.[8] Both the structural and magnetic behavior at low temperature are highly dependent on the A ion, as are the short-range magnetic correlations observed above T_N. In $ZnCr_2O_4$, the most extensively studied of the family, significant differences in properties have been observed,[7–9] but no connection has been made to the chemistry of the compound. In addition, the exact nature of the structural and magnetic ordering in $ZnCr_2O_4$ has yet to be resolved, the magnetic and structural transitions being much more complex than for $MgCr_2O_4$ and $CdCr_2O_4$. Here we report that percent level metal atom nonstoichiometry, strongly related to the synthetic conditions, can be present in both the $ZnCr_2O_4$ and $MgCr_2O_4$ spinels. In these nonstoichiometric $A_{1+x}Cr_{2-x}O_4$ compositions, excess nonmagnetic Zn or Mg is found in the Cr sites in addition to the usual A sites. To maintain charge neutrality, a corresponding fraction of Cr^{3+} is oxidized to Cr^{4+}. Thus nonstoichiometry induces both static disorder, from the presence of Zn or Mg on the Cr lattice, and dynamic disorder, through hole doping. In the case of $ZnCr_2O_4$, the magnetic properties are profoundly affected, and comparison with Ga substituted analogs, which introduce static disorder, shows that it is the hole doping, not the disorder, that has the largest impact on the magnetism.

II. EXPERIMENT

Polycrystalline samples of $A_{1+x}Cr_{2-x}O_4$ and $ACr_{2-x}Ga_xO_4$ (A = Zn, Mg, $x = 0$, 0.02, 0.04) were prepared using solid-state synthesis from high purity binary oxide starting reagents: zinc (II) oxide (Alfa Aeaser 99.99%), magnesium (II) oxide (Alfa Aeaser 99.95%), chromium (III) oxide (Fisher Scientific), and predried gallium (III) oxide (Johnson Matthey 99.999%). The appropriate quantities of reagents were intimately mixed and pressed into pellets prior to heating at 800 °C for 12 h, followed by an additional firing at 1200 °C for 24 h. This high-temperature reaction step was repeated until a phase pure product, as determined by powder x-ray diffraction, was obtained. For samples of $ZnCr_2O_4$ and $ACr_{2-x}Ga_xO_4$, the synthesis was carried out under flowing Ar gas. Synthesis of all other compositions (including $MgCr_2O_4$) was carried out in air. Samples of $ZnGa_2O_4$ and $MgGa_2O_4$ were synthesized from stoichiometric mixtures of the binary oxides heated to 1100 °C for 24 h in air.

X-ray powder-diffraction patterns were collected on a Bruker D8 Focus operating with Cu $K\alpha$ radiation and a graphite diffracted beam monochromator. High-resolution data for structural refinement were collected over the angular range $5 \leqslant 2\theta \leqslant 90^\circ$ with a step size of $\Delta 2\theta = 0.04^\circ$. Rietveld refinement[13] of the structures was carried out using the GSAS suite of programs[14] with the EXPGUI interface.[15] Backgrounds were fitted using a Chebyshev polynomial of the first kind and the peak shape was modeled using a pseudo-Voigt function.

Magnetic susceptibility and specific-heat measurements were made using a Quantum Design Physical Properties Measurement System (PPMS) and a Quantum Design MPMS-5 Superconducting Quantum Interference Device (SQUID) magnetometer. Temperature-dependent magnetization measurements of finely ground samples were collected under 0.1 and 1 T fields between 2 and 300 K after cooling in zero field. In selected samples, temperature-dependent magnetization measurements were also collected between 5 and 30 K after cooling in the measuring field (1 T). The specific heat of all samples was measured in zero field over a narrow temperature range spanning T_N, $5 \leqslant T \leqslant 15$ K. The lattice contribution to the specific heat was deducted by subtracting the specific heat of the isostructural nonmagnetic analogs, $ZnGa_2O_4$ and $MgGa_2O_4$; since no change in the symmetry of either of these phases is observed on cooling,

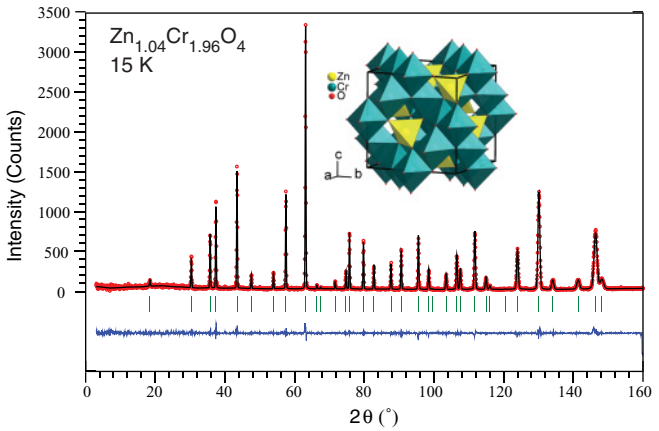

FIG. 1. (Color online) Observed (o) and calculated (-) neutron diffraction data for $Zn_{1.04}Cr_{1.96}O_4$ collected at 15 K. The difference curve is also shown; reflection positions for the cubic spinel are indicated by the vertical lines. A polyhedral model of the $ZnCr_2O_4$ structure is inset; blue (dark grey) and yellow (light grey) polyhedra represent Zn and Cr respectively.

the resultant specific heat C_{magst} includes contributions from both the magnetic and structural transitions near 12 K. Pellets for heat capacity for the Mg spinels and $ZnCr_2O_4$ were prepared by heating for 12 h at 1250 °C in the same gas as for the initial synthesis. Specific-heat measurements of nonstoichiometric and gallium-doped $ZnCr_2O_4$ were made using pressed pellets of the sample plus silver powder. The specific heat of silver was subsequently deducted.[16] Sintered pellets of the nonmagnetic analogs, $ZnGa_2O_4$ and $MgGa_2O_4$, were prepared by heating to 1150 °C for 12 h in air.

Neutron powder-diffraction patterns were collected on $ZnCr_2O_4$ and $Zn_{1.04}Cr_{1.96}O_4$ at the NIST Center for Neutron Research on the high-resolution powder neutron diffractometer (BT-1) using neutrons with wavelength $\lambda = 1.5403$ Å from a Cu(311) monochromator. Collimators with horizontal divergences of 15°, 20°, and 7° of arc were used before and after the monochromator and after the sample, respectively. Data were collected over the angular range $3 \leqslant 2\theta \leqslant 168°$ with a step size of $\Delta 2\theta = 0.05°$. Samples were placed in vanadium cans ($\phi = 10$ mm) and patterns were collected above T_N at 15 K. The intensity of selected magnetic and nuclear peaks as a function of temperature through the magnetic and structural transition was also measured. Structural refinement using the Rietveld method[13] was carried out using the FULLPROF suite of programs.[17] Backgrounds were fitted using a refined interpolation of data points and the peak shape modeled using a pseudo-Voigt function.

III. RESULTS

For both the $MgCr_2O_4$ and $ZnCr_2O_4$ systems, small amounts of metal atom nonstoichiometry are possible. At the limiting composition, $A_{1.04}Cr_{1.96}O_4$, in addition to the structural disorder introduced by A^{2+} cations on the Cr network, 2% of the Cr^{3+} is oxidized to Cr^{4+}. For both A cations, the hole doping due to the nonstoichiometry resulted in a change in color from green in the stoichiometric and Ga-doped samples to brown/black in the samples containing Cr^{4+}. What appeared to be "stoichiometric" $ZnCr_2O_4$ could be prepared in air, but, despite the absence of detectable impurity peaks in the x-ray-diffraction pattern, the brownish color and magnetic properties of the air-synthesized samples were characteristic of hole-doped nonstoichiometric $Zn_{1+x}Cr_{2-x}O_4$; only in samples prepared under an Ar atmosphere could green, stoichiometric $ZnCr_2O_4$ be prepared. In neither the nonstoichiometric nor the Ga-doped samples are distortions from the cubic spinel structure observed at room temperature; details from the x-ray refinements are given in Tables I and II. The changes to the structure on doping are small, as would be expected for such small deviations from the parent compound, and, relative to the range of lattice parameters previously reported for $ZnCr_2O_4$ [$a = 8.308$–8.330 Å (Refs. 4, 7, 12, and 18)], are insignificant. Comparison of the structural parameters obtained by refinement of the neutron-diffraction data for $Zn_{1.04}Cr_{1.96}O_4$ and $ZnCr_2O_4$ collected at 15 K (Table III and Fig. 1) shows only a small difference of the oxygen position in the two phases. This reflects a small contraction of the average $(Cr_{0.98}Zn_{0.02})O_6$ octahedral site in $Zn_{1.04}Cr_{1.96}O_4$. No evidence for Ga/Zn or Ga/Mg mixing on the A site is observable in diffraction data from the Ga-doped samples. This type of disorder is not expected in the $ZnCr_2O_4$ case because both $ZnCr_2O_4$ and $ZnGa_2O_4$ (Ref. 19) are normal spinels, but may be possible in the $MgCr_2O_4$ case because $MgGa_2O_4$ (Ref. 20) is an inverse spinel. However, in the current study such disorder, if present, is not relevant, because neither the Cr valence nor the degree of disorder on the Cr^{3+} magnetic lattice would be impacted.

The temperature-dependent magnetic susceptibility, $\chi = dM/dT$, in the $Zn_{1+x}Cr_{2-x}O_4$ spinel changes significantly (Fig. 2) with nonstoichiometry. All samples show an antiferromagnetic transition, T_N, defined by a maximum in $d(\chi T)/dT$, near 12 K (Table I). No irreversibility between the zero-field-cooled (ZFC) and field-cooled (FC) magnetic susceptibility in either of the limiting compositions is observed, and thus this small level of nonstoichiometry and/or disorder does not inhibit long-range magnetic ordering. A decrease in T_N is observed in both the hole- and Ga-doped samples. This effect is most dramatic in the nonstoichiometric hole-doped samples,

TABLE I. Structural and magnetic parameters for nonstoichiometric and Ga-doped $ZnCr_2O_4$.

	a/Å	O position/x	T_N/K	C/emu Oe^{-1} mol$_{Cr}^{-1}$K^{-1}	μ_{eff}/μ_B per Cr	θ/K
$ZnCr_2O_4$	8.31948(14)	0.2622(2)	12.6(1)	1.83	3.82	−400
$Zn_{1.02}Cr_{1.98}O_4$	8.32166(10)	0.2623(2)	11.0(1)	1.91	3.91	−373
$Zn_{1.04}Cr_{1.96}O_4$	8.32055(13)	0.2635(3)	10.8(1)	1.92	3.91	−372
$ZnCr_{1.98}Ga_{0.02}O_4$	8.3180(2)	0.2613(4)	12.4(1)	1.88	3.88	−374
$ZnCr_{1.96}Ga_{0.04}O_4$	8.3194(4)	0.2599(4)	12.4(1)	1.95	3.95	−386

TABLE II. Structural and magnetic parameters for nonstoichiometric and Ga-doped $MgCr_2O_4$.

	a/Å	O position/x	T_N/K	C/emu Oe^{-1} mol$_{Cr}^{-1}$K^{-1}	μ_{eff}/μ_B per Cr	θ/K
$MgCr_2O_4$	8.32768(11)	0.2591(3)	12.8(1)	1.97	3.97	−433
$Mg_{1.02}Cr_{1.98}O_4$	8.32789(12)	0.2562(2)	12.9(1)	1.94	3.94	−419
$Mg_{1.04}Cr_{1.96}O_4$	8.32674(11)	0.2585(2)	12.4(1)	1.92	3.93	−409
$MgCr_{1.98}Ga_{0.02}O_4$	8.3280(2)	0.2553(2)	11.9(1)	1.91	3.91	−421
$MgCr_{1.96}Ga_{0.04}O_4$	8.3263(2)	0.2553(3)	10.5(1)	1.89	3.89	−412

where a shift of 1.8 K relative to stoichiometric $ZnCr_2O_4$ ($T_N = 12.6$ K) is observed in $Zn_{1.04}Cr_{1.96}O_4$ ($T_N = 10.8$ K). The equivalent Ga substituted compound, $ZnCr_{1.96}Ga_{0.04}O_4$, in which only structural disorder is introduced, shows a much smaller and barely significant decrease in T_N, to 12.4 K. At temperatures just above T_N the magnetization when compared to $ZnCr_2O_4$ is larger in all of the doped samples. This effect is more pronounced for the nonstoichiometric materials. In nonstoichiometric $Zn_{1+x}Cr_{2-x}O_4$ the shape of the feature at T_N changes, showing a large increase in magnetization just above the transition and a sharper more pronounced decrease in χ at T_N. At high temperature, $150 \leqslant T \leqslant 300$ K, fits to the Curie-Weiss law, $\chi - \chi_o = C/T - \theta$, were carried out and are detailed in Table I. The changes on doping are relatively small, though in all the doped samples a small decrease in the Weiss temperature, θ, is observed. No significant changes to the effective moment per Cr, μ_{eff}, are observed on doping, as is expected given the small percentage of Cr^{4+} introduced by nonstoichiometry.

The changes in the magnetic susceptibility of nonstoichiometric and doped $MgCr_2O_4$ are less dramatic (Fig. 3) than for $ZnCr_2O_4$. The transition temperature T_N is observed to be highly dependent on the composition (Table II). Opposite to the shift observed in T_N for the Zn spinels, nonstoichiometry results in a smaller decrease in T_N when compared to the Ga-substitution-induced structural disorder. In the case of $Mg_{1.02}Cr_{1.98}O_4$ no significant deviation from T_N in stoichiometric $MgCr_2O_4$ is observed. As for the Zn analogs, the absence of hysteresis between the ZFC and FC susceptibility indicates the presence of long-range ordering. Around T_N the susceptibilities for the nonstoichiometric, hole-doped, and disordered Ga-doped samples are very similar, the exception being the most nonstoichiometric material $Mg_{1.04}Cr_{1.96}O_4$, where the deviations from Curie-Weiss behavior above T_N are reminiscent of those observed in $Zn_{1+x}Cr_{2-x}O_4$. The similarities between nonstoichiometric and Ga-doped samples are also seen in the magnetic parameters obtained from fitting to the Curie-Weiss law for $150 \leqslant T \leqslant 300$ K.

By rearranging the Curie-Weiss law to give, for an antiferromagnet, $C/\chi|\theta| = T/|\theta| + 1$, it can be seen that in a plot of the normalized inverse susceptibility, $C/\chi|\theta|$, as a function of normalized temperature, $T/|\theta|$, perfect Curie-Weiss behavior would result in a slope of gradient 1 intersecting the y axis at 1. Such plots have been used in comparing the behavior of geometrically frustrated magnets,[21–23] allowing differences in the nature of correlations above T_N to be identified and as a meaningful way to compare magnetic susceptibilities with significant differences in magnitude. Normalized inverse susceptibility plots are shown for the doped and nonstoichiometric $ZnCr_2O_4$ and $MgCr_2O_4$ systems in Fig. 4. These plots show that the magnetic susceptibility is dependent on both the type of dopant and the A ion. The large degree of frustration in all of the spinels can be seen in the suppression of the ordering

TABLE III. Structural parameters and bond lengths of $ZnCr_2O_4$ and $Zn_{1.04}Cr_{1.96}O_4$ from neutron powder diffraction at 15 K.

15 K		$ZnCr_2O_4$	$Zn_{1.04}Cr_{1.96}O_4$
Space group		$Fd\bar{3}m$	$Fd\bar{3}m$
a/Å		8.320721(5)	8.321816(6)
R_f		1.12	1.49
χ^2		1.24	1.24
Zn	B_{iso}/Å^2	0.16(2)	0.20(3)
8a			
$(\frac{1}{8},\frac{1}{8},\frac{1}{8})$			
Cr/Zn	B_{iso}/Å^2	0.13(2)	0.25(3)
16d			
$(\frac{1}{2},\frac{1}{2},\frac{1}{2})$			
O	x	0.26157(3)	0.26169(5)
32e	B_{iso}/Å^2	0.21(1)	0.28(2)
(x, x, x)			
Zn-O/Å		1.9717(3)	1.9737(4)
Cr/Zn-O/Å		1.9921(3)	1.9914(4)
Cr/Zn-Cr/Zn/Å		2.9469786(1)	2.9473624(1)

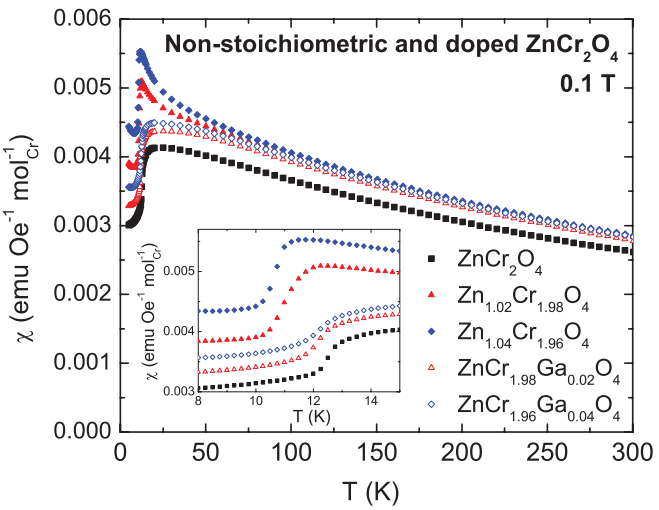

FIG. 2. (Color online) Magnetic susceptibility (χ) as a function of temperature for samples of nonstoichiometric and doped $ZnCr_2O_4$; the inset shows the magnetic susceptibility around T_N in more detail. Closed symbols represent nonstoichiometric $Zn_{1+x}Cr_{2-x}O_4$ and open symbols represent doped $ZnCr_{2-x}Ga_xO_4$.

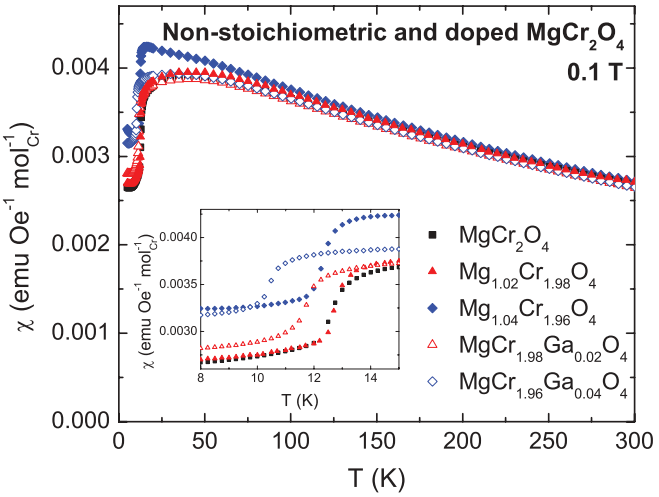

FIG. 3. (Color online) Magnetic susceptibility (χ) as a function of temperature for samples of nonstoichiometric and doped $MgCr_2O_4$; the inset shows the magnetic susceptibility around T_N in more detail. Closed symbols represent nonstoichiometric $Mg_{1+x}Cr_{2-x}O_4$ and open symbols doped $MgCr_{2-x}Ga_xO_4$.

temperature $T_N/|\theta| \sim 0.03$ (typically for a frustrated system $T_N/|\theta| < 0.1$). In stoichiometric $ZnCr_2O_4$, antiferromagnetic short-range correlations, i.e., positive deviations from Curie-Weiss behavior, are observed above T_N. However, ferromagnetic short-range correlations, i.e., negative deviations from Curie-Weiss behavior, are observed in the nonstoichiometric hole-doped compositions. The Ga-doped samples of $ZnCr_2O_4$ exhibit stronger antiferromagnetic short-range correlations than the stoichiometric phase. Comparison of the normalized susceptibility for $Zn_{1.04}Cr_{1.96}O_4$ and $ZnCr_{1.96}Ga_{0.04}O_4$ shows a dramatic difference: for static disorder on the Cr lattice, enhanced antiferromagnetic correlations are induced above T_N, while disorder and hole doping enhances the ferromagnetic correlations. Curiously, one can infer from Fig. 4 that for nonstoichiometry near $Zn_{1.04}Cr_{1.96}O_4$, the induced ferromagnetic and intrinsic antiferromagnetic short-range correlations compensate for one another, giving apparently ideal Curie-Weiss-like behavior to lower $T/|\theta|$ than for the stoichiometric material. In the $MgCr_2O_4$ system both nonstoichiometric and doped compositions display positive deviations from the Curie-Weiss law above T_N indicative of antiferromagnetic short-range correlations. The onset temperature of the correlations appears to be independent of whether the dopant induces disorder or both disorder and hole doping.

Specific-heat measurements are shown in Figs. 5 and 6. The specific heat allows the changes in entropy resulting from the structural and magnetic transitions to be probed. For an antiferromagnet, changes to the magnetic entropy, as reflected in the specific heat, have similar behavior to $d(\chi T)/dT$.[24] On consideration of the specific heat it can be seen that in both the doped $ZnCr_2O_4$ and $MgCr_2O_4$ systems the peaks in the specific heat and the magnetic entropy, $d(\chi T)/dT$, are coincident. This indicates that the structural and magnetic transitions occur simultaneously, as some part of the specific-heat anomaly must be due to the structural phase transition.

In nonstoichiometric $MgCr_2O_4$ the decrease in the temperature of the transitions is small, and as the nonstoichiometry increases a broadening in the peak in the specific heat is observed. A larger shift in the transition temperature is observed in the Ga-doped samples; from $T_N = 12.4$ K in stoichiometric $MgCr_2O_4$ to $T_N = 10.5$ K in $MgCr_{1.96}Ga_{0.04}O_4$. In contrast, in nonstoichiometric $Zn_{1+x}Cr_{2-x}O_4$ (Fig. 5) the

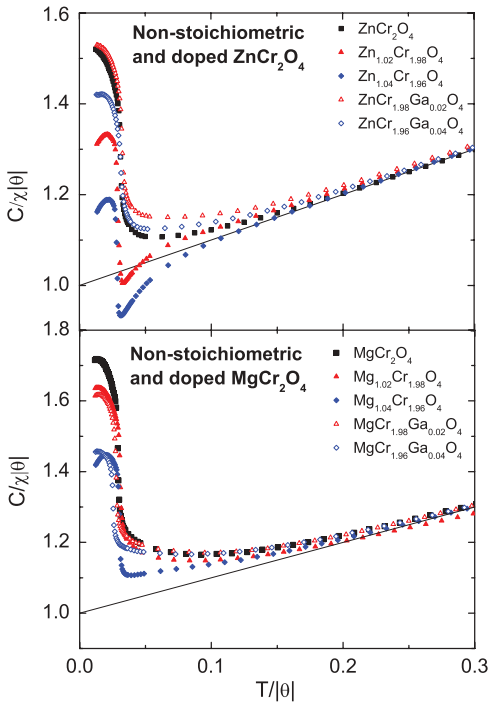

FIG. 4. (Color online) Normalized inverse susceptibility plots for nonstoichiometric and doped $ZnCr_2O_4$ (upper) and $MgCr_2O_4$ (lower).

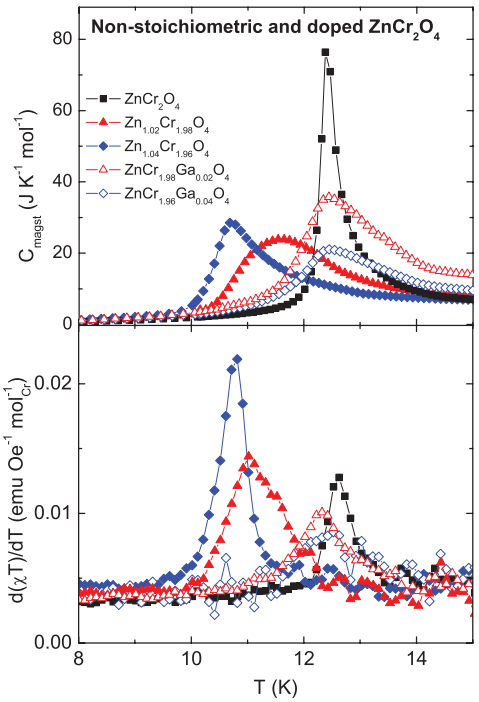

FIG. 5. (Color online) Magnetic contribution to the specific heat in nonstoichiometric and doped $ZnCr_2O_4$. The lower panel shows the differential of the magnetic entropy, $d(\chi T)/dT$.

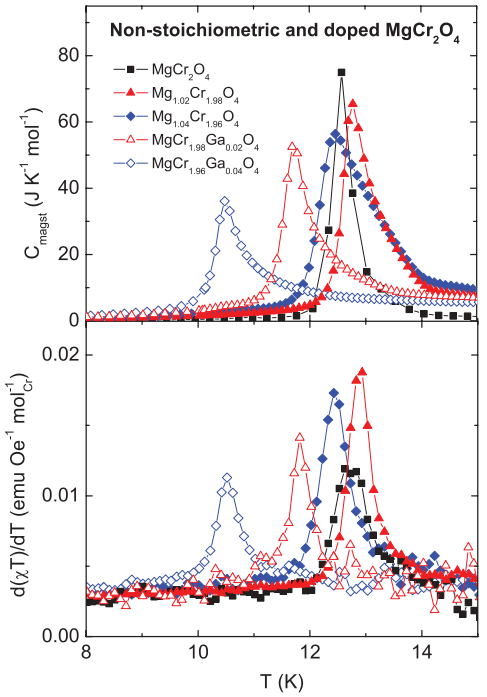

FIG. 6. (Color online) Magnetic contribution to the specific heat in nonstoichiometric and doped $MgCr_2O_4$. The lower panel shows the differential of the magnetic entropy, $d(\chi T)/dT$.

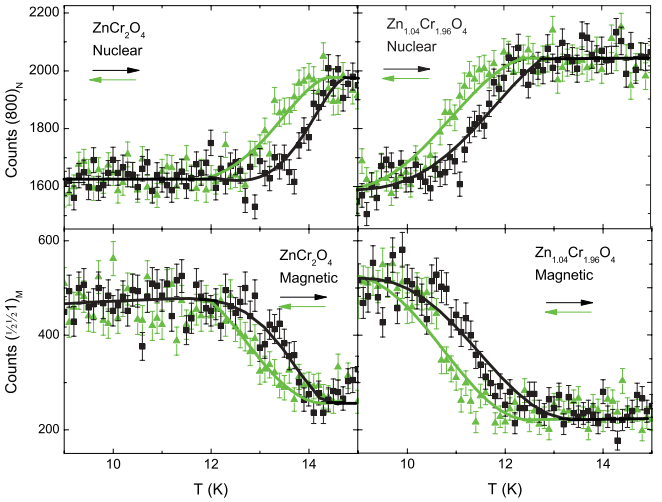

FIG. 7. (Color online) Evolution of the nuclear reflection $(800)_N$ (upper) and the magnetic $(\frac{1}{2}\ \frac{1}{2}\ 1)_M$ reflection (lower) as a function of temperature in $ZnCr_2O_4$ (left) and $Zn_{1.04}Cr_{1.96}O_4$ (right). Data are shown for both warming (black squares) and cooling (green triangles). The solid lines are a guide to the eye.

maxima in the specific heat shift to dramatically lower temperatures as the nonstoichiometry increases. A smaller decrease in temperature is observed in the Ga-doped samples. For both nonstoichiometric and Ga-doped $ZnCr_2O_4$ the broadening of the transitions observed in the specific heat and the magnetic entropy indicate a more diffuse magnetic transition relative to stoichiometric $ZnCr_2O_4$ and the nonstoichiometric or doped $MgCr_2O_4$ systems. The origin of the more diffuse transition is not currently known, however, if the phase transition indeed results from small structural changes that break the symmetry of otherwise frustrating interactions,[6] it is plausible that small changes in stoichiometry or disorder impact the detailed character of the transitions significantly.

To investigate the changes in the structure and magnetic ordering in $Zn_{1-x}Cr_{2-x}O_4$ at $\sim T_N$ in more detail, low-temperature neutron-diffraction data were collected on $Zn_{1.04}Cr_{1.96}O_4$ and $ZnCr_2O_4$. On cooling below T_N, magnetic peaks appear in the diffraction patterns, and a broadening of the $(800)_N$ nuclear reflection, indicative of a reduction in structural symmetry, is observed. The structural and magnetic transitions were investigated by following the evolution of peaks that show a change in intensity associated only with the individual transitions (Fig. 7); for the nuclear transition this is the $(800)_N$ reflection at $2\theta \sim 96^\circ$ and for the magnetic transition a peak indexed as $(\frac{1}{2}\ \frac{1}{2}\ 1)_M$ at $2\theta \sim 22.6^\circ$ using the supercell proposed by Ji *et al.*[6] As in the magnetic susceptibility and specific heat a clear decrease in the temperature of the structural and magnetic transitions is observed in $Zn_{1.04}Cr_{1.96}O_4$ compared to $ZnCr_2O_4$. For both compositions, the onset of the structural and magnetic transitions is the same within the precision of the measurement. Thus the structural and magnetic transitions are coupled in both the stoichiometric and the nonstoichiometric compounds. Since no irreversibility between the ZFC and FC susceptibility is observed in either $ZnCr_2O_4$ or $Zn_{1.04}Cr_{1.96}O_4$ the hysteresis observed in the evolution of the structural and magnetic transitions at T_N from neutron diffraction may be a result of the finite thermal sweep rate during the diffraction measurements.

IV. DISCUSSION AND CONCLUSION

Nonstoichiometry and the resultant hole doping in $ZnCr_2O_4$ and $MgCr_2O_4$ spinels has a profound effect on the magnetic properties even at a doping level of 2% or lower. The low-temperature behavior is highly dependent on both the A ions and the type of dopant. In nonstoichiometric $Zn_{1+x}Cr_{2-x}O_4$ the changes observed are complex. The change in the nature of the correlations above T_N in the nonstoichiometric hole-doped samples is the most significant indication of the effect of hole doping on the magnetic properties. These correlations above T_N are indicative of short-range ordering and, due to the magnetostructural coupling, are expected to play a role in the formation of both the crystallographic and magnetic long-range-ordered states below T_N. The presence of short-range ferromagnetic correlations above T_N in nonstoichiometric $Zn_{1+x}Cr_{2-x}O_4$ may therefore be indicative of a change in the magnetic or/and structural ordering at lower temperatures. $MgCr_2O_4$ appears to be more robust, with smaller though significant changes in behavior induced by nonstoichiometry. This is consistent with the simpler structural and magnetic ordering transition observed in stoichiometric $MgCr_2O_4$. We have not studied the structure of doped or nonstoichiometric $MgCr_2O_4$ below T_N, but the relatively small systematic changes to the magnetization and the specific heat suggest that the magnetic and structural characteristics are similar to that of stoichiometric $MgCr_2O_4$. The coincidence of the peaks in the specific heat and $d(\chi T)/dT$ indicates that the structural and magnetic transitions occur simultaneously in both $MgCr_2O_4$ and $ZnCr_2O_4$, and thus small levels of

doping or nonstoichiometry are not sufficient to disrupt the coupling of the structural and magnetic transitions. Thus, as for the stoichiometric case, it can be inferred that in doped $MgCr_2O_4$ and $ZnCr_2O_4$ spin-lattice coupling drives the concurrent structural and magnetic transitions at low temperature. This single transition occurs at a temperature where the magnetic interactions overcome the stiffness of the lattice; at that temperature a lattice distortion sets in, decreasing the symmetry, relieving the magnetic frustration, and allowing magnetic ordering. In the nonstoichiometric and Ga-doped systems both the structure and the magnetic network are disrupted by the presence of the small number of "impurity atoms" and it may be that it is through impacting the lattice stiffness that hole doping, nonstoichiometry, and disorder change T_N. Rationalizing the changes in T_N thus requires comprehending in more detail the changes in both the structural and magnetic regimes introduced by the introduction of Ga or nonstoichiometry.

Because the sizes of the magnetic lattices in $MgCr_2O_4$ and $ZnCr_2O_4$ are very similar, the difference in magnetic properties of $MgCr_2O_4$ and $ZnCr_2O_4$ cannot simply be ascribed to differences in crystal structure above T_N. Instead we speculate that they may be due to the subtle differences in bonding, and subsequently the magnetic exchange interactions, that are a consequence of the difference in electronegativity between Zn and Mg. Given the difference in the behavior of the parent compounds, it is not surprising that $ZnCr_2O_4$ and $MgCr_2O_4$ exhibit different properties when doped or nonstoichiometric. The divergence in the behavior of the doped $ZnCr_2O_4$ and $MgCr_2O_4$ spinels highlights the difficulties in generalizing the relationships between chemical perturbations to the magnetic lattice and the magnetic properties in geometrically frustrated magnets. In addition to the chromium (III) spinels, the only other hole-doped geometrically frustrated system containing Cr^{3+} reported is $\beta-CaCr_2O_4$.[21] In all three systems, hole doping induces different changes in the magnetism compared to static doping; the behavior of each individual system is also different. Thus charge doping provides an additional means of manipulating the sometimes delicate balance of interactions within geometrically frustrated magnetic systems.

ACKNOWLEDGMENTS

The authors wish to thank Shuang Jia and E. Climent-Pascual for their helpful discussions. This research was supported by the US Department of Energy, Division of Basic Energy Sciences, Grant No. DE-FG02-08ER46544.

*sdutton@princeton.edu

[1] A. Apostolov, M. Michov, Z. Charizanova, K. Zaveta, C. Christoy, and P. Colakov, Czech. J. Phys. **34**, 46 (1984).
[2] C. Battistoni, J. L. Dormann, D. Fiorani, E. Paparazzo, and S. Viticoli, Solid State Commun. **39**, 581 (1981).
[3] H. Ehrenberg, M. Knapp, C. Baehtz, and S. Klemme, Powder Diffr. **17**, 230 (2002).
[4] D. Fiorani, S. Viticoli, J. L. Dormann, J. L. Tholence, J. Hammann, A. P. Murani, and J. L. Soubeyroux, J. Phys. C **16**, 3175 (1983).
[5] V. N. Glazkov, A. M. Farutin, V. Tsurkan, H. A. Krug von Nidda, and A. Loidl, Phys. Rev. B **79**, 024431/1 (2009).
[6] S. Ji, S. H. Lee, C. Broholm, T. Y. Koo, W. Ratcliff, S. W. Cheong, and P. Zschack, Phys. Rev. Lett. **103**, 037201/1 (2009).
[7] I. Kagomiya, H. Sawa, K. Siratori, K. Kohn, M. Toki, Y. Hata, and E. Kita, Ferroelectrics **268**, 327 (2002).
[8] S. H. Lee *et al.*, J. Phys.: Condens. Matter **19**, 145259/1 (2007).
[9] S. H. Lee, W. Ratcliff II, Q. Huang, T. H. Kim, and S. W. Cheong, Phys. Rev. B **77**, 014405/1 (2008).
[10] H. Martinho *et al.*, Phys. Rev. B **64**, 024408 (2001).
[11] L. Ortega-San-Martin, A. J. Williams, C. D. Gordon, S. Klemme, and J. P. Attfield, J. Phys.: Condens. Matter **20**, 104238 (2008).
[12] Y. Xue, S. Naher, F. Hata, H. Kaneko, H. Suzuki, and Y. Kino, J. Low Temp. Phys. **151**, 1193 (2008).
[13] H. M. Rietveld, J. Appl. Crystallogr. **2**, 65 (1969).
[14] A. C. Larson and R. B. Von Dreel, Los Alamos National Laboratory Report No. LAUR 86–748, 1994.
[15] B. H. Toby, J. Appl. Crystallogr. **34**, 210 (2001).
[16] D. R. Smith and F. R. Fickett, J. Res. Natl. Inst. Stand. Technol. **100**, 119 (1995).
[17] J. Rodríguez-Carvajal, Physica B **192**, 55 (1993).
[18] S. Klemme and J. C. van Miltenburg, Mineral. Mag. **68**, 515 (2004).
[19] J. Hornstra and E. Keulen, Philips Res. Rep. **27**, 76 (1972).
[20] M. Huber, J. Chim. Phys. **57**, 202 (1960).
[21] S. E. Dutton, C. L. Broholm, and R. J. Cava, J. Solid State Chem. **183**, 1798 (2010).
[22] G. C. Lau, T. Klimczuk, F. Ronning, T. M. McQueen, and R. J. Cava, Phys. Rev. B **80**, 214414 (2009).
[23] B. C. Melot, J. E. Drewes, R. Seshadri, E. M. Stoudenmire, and A. P. Ramirez, J. Phys.: Condens. Matter **21**, 216007 (2009).
[24] M. E. Fisher, Philos. Mag. **7**, 1731 (1962).